Article

High Crystallinity Covalent Organic Framework with Dual Fluorescence Emissions and its Ratiometric Sensing Application

Hai-Long Qian, Cong Dai, Cheng-Xiong Yang, and Xiu-Ping Yan

ACS Appl. Mater. Interfaces, **Just Accepted Manuscript** • DOI: 10.1021/acsami.7b08060 • Publication Date (Web): 28 Jun 2017

High Crystallinity Covalent Organic Framework with Dual Fluorescence Emissions and its Ratiometric Sensing Application

Hai-Long Qian,[a,b] Cong Dai,[c] Cheng-Xiong Yang[c] and Xiu-Ping Yan*[,a,b,c,d]

[a] State Key Laboratory of Food Science and Technology, Jiangnan University, Wuxi 214122, China

[b] Institute of Analytical Foodsafetiology, School of Food Science and Technology, Jiangnan University, Wuxi 214122, China

[c] Research Center for Analytical Sciences, Tianjin Key Laboratory of Molecular Recognition and Biosensing, College of Chemistry, Nankai University, 94 Weijin Road, Tianjin 300071, China

[d] Collaborative Innovation Center of Chemical Science and Engineering (Tianjin), 94 Weijin Road, Tianjin 300071, China

*E-mail: xpyan@nankai.edu.cn; xpyan@jiangnan.edu.cn

ABSTRACT

Highly crystallinity of covalent organic frameworks (COFs) with dual fluorescence emissions has not been reported so far. Here we show the rational design and preparation of high crystallinity COF TzDa via the synergetic interaction of docking sties and hydrogen bonds. 4,4',4''-(1,3,5-Triazine-2,4,6-triyl)trianiline (Tz) with the docking site and 2,5-dihydroxyterephthalaldehyde (Da) with OH group are employed to synthesize the imine-linked two-dimensional high crystallinity layered structure TzDa. The prepared mesoporous TzDa (ca. 36 Å) exhibits high thermal and chemical stability. The intramolecular charge transfer (ICT) and excited state intramolecular proton transfer (ESIPT) effects bring TzDa two main fluorescence emissions around 500 nm and 590 nm. Water molecules can interfere with the ICT and ESIPT effects, allowing developing a ratiometric fluorescent sensor for water in organic solvent. The proposed sensor shows high sensitivity to trace water in conventional organic solvents. The high stability of TzDa allows its recyclable uses for trace water detection. This work not only offers a platform for the construction of high crystallinity COFs, but also provides a rational design of COFs with dual fluorescent emissions for ratiometric sensing application.

KEYWORDS: *covalent organic framework, high crystallinity, dual fluorescence emissions, ratiometric sensing, trace water*

INTRODUCTION

Covalent organic frameworks (COFs) is new emerging type of crystalline porous polymer, and gains great concern in recent years.[1-5] Construction of light elements and strong covalent bonds with highly regular structures offers COFs inherent porosity with low density, high stability and large surface area.[6-11] The utilization of the COFs focuses in catalysis,[12-14] photoconduction,[15-17] gas storage[18-20] and separation.[21,22] Recently, Wang's group and Jiang's group brought a new application area of COFs in sensing.[23,24] As a crystalline materials, enhancing the crystallinity of COFs remains a challenge in preparing high quality of COFs.[25] General strategies to improve the crystallinity of COFs are to introduce either hydrogen bonds to increase intralayer interaction and layer planarity,[16,26-28] or docking sites with lock-and-key-like central units to guide the attachment of the successive layers.[25,29]

Detection of moisture content in organic solvents is always an important process in many chemical and industrial productions because water content directly influences the yield and selectivity of numerous sensitive chemical reactions.[30] Although traditional analytical techniques for detection of trace water, such as Karl Fischer titration and chromatography, show ppm level water detection with high accuracy, they own some shortcomings (use of toxic reagents, long analysis time and tedious operation). Recently, luminescence-based sensors have been developed to detect trace water with different kinds of fluorogenic probes,[30,31] luminescent metal nanoclusters[32] and metal organic frameworks.[33] However, most of these reported sensors only provide intensity-varying signals of single fluorescence, which likely be interfered by

intensity of excitation, collection efficiency of emission signal, and inhomogeneous distribution of probe.[34] Besides, they cannot be recycled for use due to their hard separation from water or instability.

Herein, we report the rational designed synthesis of a high crystallinity COF with dual fluorescence emissions for ratiometric sensing of trace water in organic solvents via a synergetic approach of docking sites and hydrogen bonds. We chose the 4,4',4''-(1,3,5-Triazine-2,4,6-triyl)trianiline (Tz) and 2,5-dihydroxyterephthalaldehyde (Da) as the ligands to synthesize a high crystallinity COF TzDa where the Tz offers the docking sites and the Da provides the hydrogen bonds. The mesoporousTzDa possesses high stability and large surface area. The Tz moiety brings TzDa structure an intramolecular charge transfer (ICT) effect while the hydrogen interactions between the Da and imines results in excited state intramolecular proton transfer (ESIPT) effect. As a result, the TzDa gives two main fluorescence emissions around 500 nm and 590 nm. On the basis of the effect of water on ICT and ESIPT, we develop a ratiometric fluorescent sensor for detecting trace water in organic solvents with high sensitivity and selectivity as well as excellent reusability.

EXPERIMENTAL SECTION

Synthesis of COF TzDa. A 35 mL Schlenk tube (OD 26 × L 125 mm) was charged with Tz (31.9 mg, 0.09 mmol), Da (21.6 mg, 0.13 mmol), o-dichlorobenzene (o-DCB, 1.8 mL), N,N-dimethylacetamide (DMAC, 0.2 mL) and 6 M aqueous acetic acid (0.2 mL). After 10 min sonication, the tube was frozen with liquid nitrogen bath, degassed through three freeze–pump–thaw cycles, sealed with the screw cap and

heated at 120 °C for 3 d. The formed dark red product was collected via centrifugation and rinsed with tetrahydrofuran (THF). The isolated powder was then extracted with dichloromethane (DCM) and dried at 100 °C under vacuum for 24 h to obtain TzDa in ca.88 % isolated yield. Fourier transform-infrared spectroscopy (FTIR): 3432, 1614, 1579, 1511, 1411, 1363, 1208, 1175, 1146 cm^{-1}. Anal. Calcd. for $(C_{10}H_7N_2O)n$: C 70.18; H 4.09; N 16.37. Found: C 70.02; H 3.98; N 16.04. Powder X-ray diffraction (PXRD): 2.9°, 4.9°, 5.8°, 7.5°, 8.8°, 25.9°.

Structural Simulation and PXRD Analysis. Structure modeling of the TzDa was conducted with Material Studio (ver. 7.0) suite of programs by Accelrys. According to the previous work,[27] the initial lattice was generated with the space group P6/m (a = b = 36.2000 Å, c = 3.4000 Å), and the unit cell was defined by two Tz molecules bond to Da via six hydrazine linkages. After geometry optimization using MS Forcite molecular module (Universal force fields, Ewald summations), the crude structure modeling of the TzDa was obtained. Subsequently, pawley refinement was applied to obtain the refined PXRD profile with the lattice parameters of a = b = 36.1922 Å, c = 3.4399 Å, Rwp = 6.92%, Rp = 4.99%. Moreover, a staggered arrangement for TzDa as an alternative structure was also performed wherein the initial lattice was generated with the space group P63/m (a = b = 36.1922 Å, c = 6.8800 Å).

Stability Test. 10 mg of the COF samples were immersed in 1 mL of THF, acetone, acetonitrile (ACN), ethanol, ethyl acetate (EtAC), isopropanol (IPA) or water for 5 days. Then, the samples were rinsed with THF and DCM, dried under vacuum at

100 °C for 24 h and offered to PXRD characterization. Besides, the 10 mg TzDa samples were heated under air at 200 °C, 250 °C, 300 °C and 350 °C for 3 h, then offered to PXRD characterization.

Ratiometric Detection of Water in Organic Solvents. Certain amount ofTzDa (1.000 mg) was ultrasonically dispersed in 10 mL organic solvent samples. 1 mL of the above obtained sample solution was added to a clean quartz cell (1 × 1 cm) with a slight shaking. The corresponding fluorescence spectra upon excitation at 365 nm were recorded for subsequent fluorescent ratiometric detection of water.

RESULTS AND DISCUSSION

Design, Preparation and Characterization of the COFs. Figure 1 shows the design and synthesis of COF TzDa. So far, two strategies, either introducing hydrogen bonds to increase intralayer interaction and layer planarity[25,26] or docking sites to guide the attachment of the successive layer,[27] have been developed to prepare high crystallinity COFs. Here we introduced an approach to integrate the above two strategies to synthesize high crystallinity COF TzDa (Figure 1b). For this purpose, we used Tz and Da as the ligands. Tz is a typical screw-shaped molecule and this kind of structure with docking sites can significantly preclude error-prone network formation during the preparation of COFs. Moreover, Da can provide OH group to offer strong intramolecular hydrogen bonding interactions with the imine nitrogen to lock the phenyl rings and amplify the interactions among the adjacent layers.

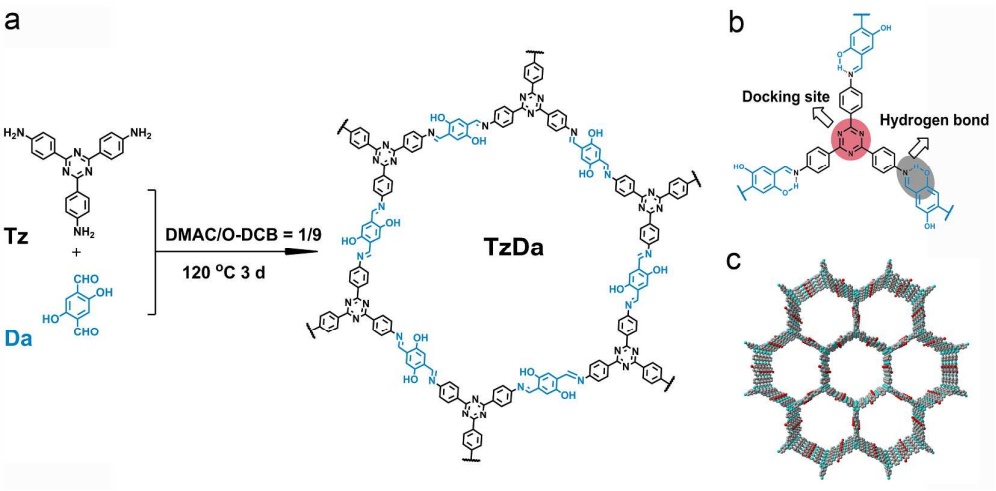

Figure 1. (a) Construction of TzDa via the condensation of Tz and Da. (b) Illustration of the docking sites and hydrogen bond of TzDa. (c) Graphic view of TzDa for the AA eclipsed model (grey, C; cyan, N; red, O; H is omitted for clarity).

The present combined approach of the two strategies gave a high crystallinity COF TzDa. The PXRD pattern shows a high intense peak at 2.9° and other minor peaks at 4.9°, 5.8°, 7.5°, 9.8°, 25.9° corresponding to the strong reflection from 100 and 110, 200, 120, 220, 001 plane, respectively (Figure 2a, red line). Such specific peaks are rarely seen in Schiff-base type COFs.[35-38] The stacking distances of the adjacent layers were determined to be ca. 3.4399 Å from the d spacing (Figure 2a insert) according to the Bragg's law.[39] The above results reveal the high crystallinity of the prepared TzDa.

We also prepared a TRITER-1 COF with Tz and terephthaldehyde as the ligands according to Gomes[40] for comparison (Figure S1-S4). In this case, Tz can still provide the docking sites whereas terephthaldehyde cannot offer the OH group for hydrogen bonding. As a result, we obtained poor crystallinity of TRITER-1 (Figure S2). The above result indicates only the docking sites without the hydrogen bonds cannot bring

high crystallinity of the COF and the synergetic effect of the docking sites and hydrogen bonding plays a critical importance in the preparation of high crystallinity of the COF.

Two kinds of two-dimensional (2D) models (eclipsed AA and staggered AB) were generated by Materials Studio (ver. 7.0) to investigate the possible structure of TzDa (Figure 2b and 2c; Figure S5 and S6). Compared with the PXRD pattern of staggered AB model, those of the eclipsed AA mode generated with a space group P6/m ($a = b = 36.1922$ Å, $c = 3.4399$ Å, $\alpha = \beta = 90°$ and $\gamma = 120°$) shows more agreement with the experimental pattern with Rwp of 6.92% and Rp of 4.99% after pawley refinement (Figure 2a; Figure S7 and Table S1), indicating that the structure of the prepared TzDa mainly matches an eclipsed AA stacking 2D material.

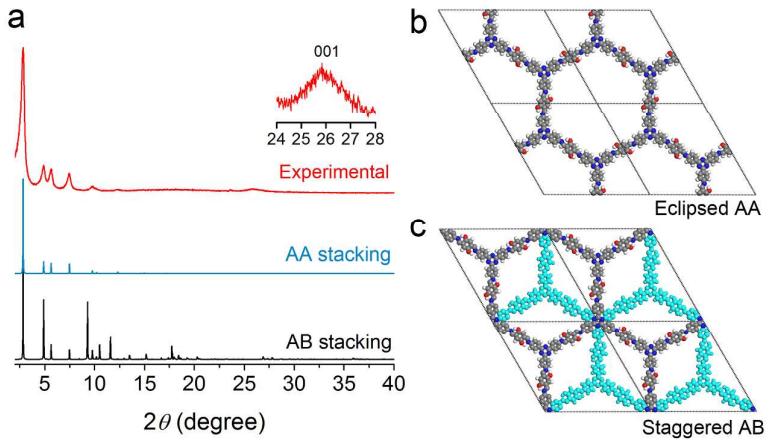

Figure 2. (a) PXRD pattern of TzDa: experimental pattern (red curve); simulated pattern for the AA eclipsed model (blue curve) and AB staggered model (black curve). (b) Eclipsed unit cell of TzDa. (c) Staggered unit cell of TzDa.

The TzDa gave a new characteristic peak of the stretching band of C=N at 1614 cm^{-1} in Fourier transform-infrared (FTIR) spectra other than those of Tz and Da

(Figure 3a), revealing the formation of imine bonds. The absence of some characteristic peaks of the starting ligands (C=O at 1664 cm^{-1} of Da and N-H at ca. 3300 cm^{-1} of Tz) further proves the occurrence of the Schiff-base reaction. ^{13}C CP-MAS solid-state nuclear magnetic resonance (NMR) spectroscopy gave more specific structure information of the TzDa. The carbon chemical shift of the C=O on Da was 200 (Figure S8). After condensation reaction, the corresponding carbon chemical shift on TzDa changed to 160 (the carbon peak of the C=N, Figure 3b), indicating the successful construction of imine bonds. The other chemical shifts for the rest carbon peaks of TzDa at 115, 122, 129, 135, 148, 153 and 169 are in good agreement with those of Tz and Da (Figure S9 and S10).

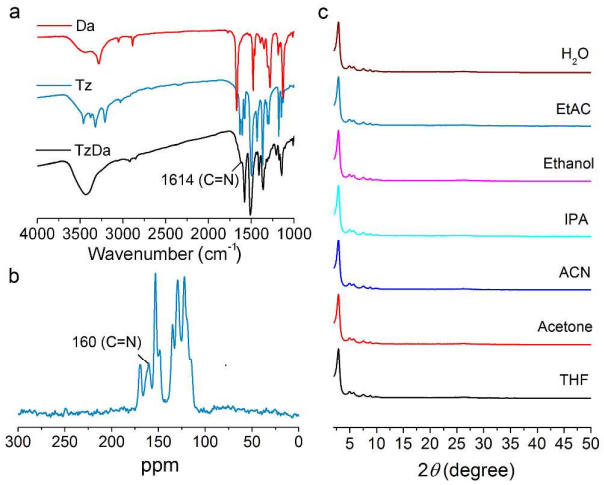

Figure 3. (a) FTIR spectra of Da, Tz and TzDa.(b) Solid-state ^{13}C NMR spectra of TzDa. (c) PXRD patterns of TzDa after treatment in different solvents.

Thermogravimetric analysis (TGA) reveals no remarkable weight loss of TzDa up to 400 °C under air condition (Figure S11). Furthermore, the PXRD pattern of TzDa heated at different temperatures in air were monitored to demonstrate the thermal stability of the crystal structure of TzDa (Figure S12). The PXRD pattern of TzDa

remained unchanged until 300 °C, showing the framework of TzDa is stable up to 300 °C. However, all the peaks of the PXRD pattern disappeared after further increase to 350 °C, indicating the framework of TzDa collapsed. TzDa is also stable in water and various organic solvents (Figure 3c).

Both scanning electron microscopy (SEM) and transmission electron microscopy (TEM) images reveal the fluffy cluster-like morphology of TzDa (Figure 4a and 4b). Further magnification of the TEM image reveals the obvious sheet structure of TzDa due to the strong π-π stacking interactions between adjacent layers (Figure S13).

The permanent porosity and Brunauer-Emmett-Teller (BET) surface areas of the activated TzDa were characterized via the N_2 adsorption–desorption analysis at 77 K (Figure 4c and Figure S14). The BET surface area of the as-prepared TzDa was 709 $m^2 g^{-1}$ and the total pore volume of TzDa was 0.53 $cm^3 g^{-1}$. The large surface area of the prepared COF was benefit from the high crystallinity of the COF. The prepared TzDa are mainly mesoporous with a main pore size of ca. 36 Å. (Figure 4d).

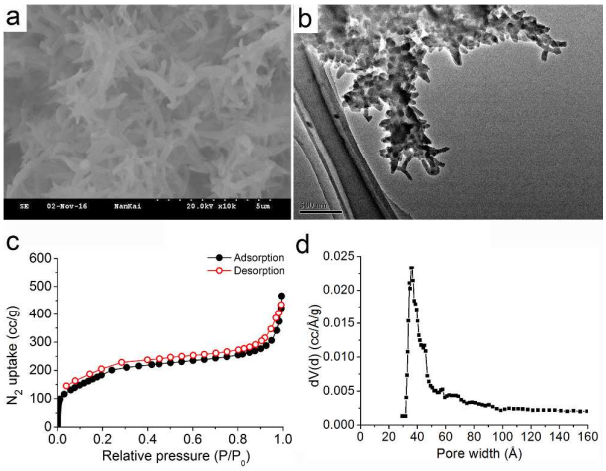

Figure. 4 (a) SEM and (b) TEM image of TzDa. (c) N_2 adsorption–desorption isotherms of TzDa. (d) Pore size distribution of TzDa.

Optical Properties of TzDa. The prepared TzDa gives absorption peaks at 365 and 425 nm, and shows two main fluorescence emissions around 500 nm and 590 nm in common organic solvents (Figure 5a and Figure S15). The main emission around 500 nm shows a slight red-shift as the solvent polarity increases owing to the intramolecular charge transfer (ICT) of Tz moiety with the phenyl group as a donor and the triazine as an acceptor.[41] Tz ligand also exhibits the same red-shift phenomenon (Figure S16). In addition, TzDa owns intramolecular hydrogen bonding interaction between the O-H on Da and the generated C=N bond. Such intramolecular hydrogen bonding leads to excited state intramolecular proton transfer (ESIPT) effect in TzDa to give a second emission at ca. 590 nm.[42] For comparison, a compound TzSa with similar structure to the unit of TzDa synthesized through the condensation of Tz and salicyldehyde only gives a single fluorescence emission (Figure S18-S20), indicating the strong π-π stacking crystallinity structure of TzDa also plays an essential role in providing the dual fluorescence emissions.

We also found the sensitive response of the dual fluorescence emissions of TzDa to trace water in organic solvents (Figure 5b and Figure S21). The increase of water content leads to the growth of the fluorescence intensity of TzDa for the longer wavelength emission (ca. 590 nm) and the reduction of that for the shorter wavelength emission (ca. 500 nm). This special phenomenon results from the interference of water to the ICT and the ESIPT effect of TzDa as shown in Figure 5c. On the one hand, the hydrogen bonding interaction between water (as a hydrogen bond donor) and Tz moiety (as a hydrogen bond acceptor) would block the ICT process from

triazine to the phenyl group, increasing the possibility of nonradiative relaxation of TzDa. Thus, the fluorescence emission intensity at ca. 500 nm would decrease.[43,44] On the other hand, the water also interacts with the OH group on the Da, breaking the intramolecular hydrogen bonding between the OH and the generated C=N. Consequently, the changed exited state form of the hydroxyl group in Da moiety increases the fluorescence emission intensity at ca. 590 nm.[45,46]

Fluorescence experiments were performed on the control COF DhaTab and TRITER-1 to further support the above explanation for the effect of water on the fluorescence of TzDa. The COF DhaTab was synthesized with 1,3,5-tris(4-aminophenyl)benzene (Tab) and Da (Figure S22-S25).[27] DhaTab and TzDa have similar structure, but the former has no triazine group in Tab while the later possesses the triazine group in Tz. Owing to the absence of the triazine group in Tab, DhaTab has no ICT effect. The only ESIPT effect in DhaTab leads to the only one emission at ca. 590 nm of DhaTab and the growth of the fluorescence intensity with the increase of water content (Figure S26). The COF TRITER-1 was synthesized with Tz and terephthaldehyde. TRITER-1 and TzDa also have similar structure, but the former has no OH group in terephthaldehyde while the later possesses the OH group in Da. The absence of the OH group in terephthaldehyde leads to the disappearance of ESIPT effect. Thus, the only ICT effect of TRETER-1 gives the only one emission at ca. 510 nm and the decrease of the emission intensity with the increase of water content (Figure S27).

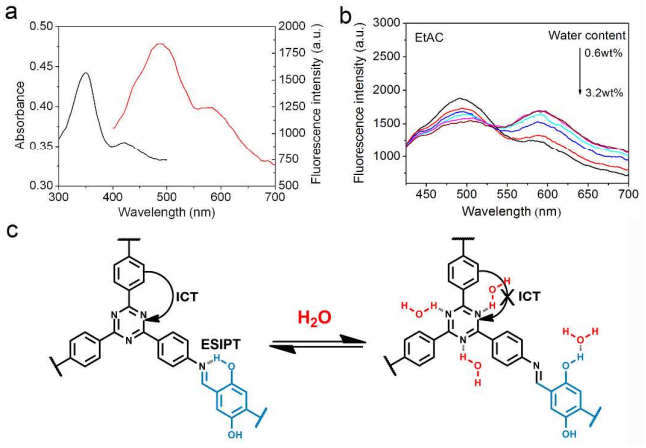

Figure. 5 (a) UV−vis absorption (black) and fluorescence (red) spectra of the TzDa in pure EtAc. (b) Fluorescence spectra of TzDa in EtAC with different water content. (c) H_2O sensing mechanism by TzDa.

Ratiometric Fluorescence Sensing of Water. The dual emissions of the prepared TzDa with ICT and ESIPT phenomena and their sensitive response to trace water in organic solvents offer the potential of TzDa as a fluorescent ratiometric probe for sensing water. To this end, we first studied the effect of ultrasonication time on the intensity ratio of the two fluoresce emissions of TzDa in various organic solvents (IPA, acetone, THF, EtAC, and ethanol) containing 10.0wt% water. The results show that the fluorescence ratio (longer wavelength emission to shorter wavelength emission) in organic solvents got stable within 1 min, revealing the quick fluorescence response of TzDa to water (Figure S28). In addition, the ratio of the two fluorescence emissions of TzDa linearly increases with the water content in organic solvents IPA, acetone, THF, EtAC and ethanol in a range of 1.1wt% - 7.7wt%, 0.1wt% - 5.1wt%, 0.5wt% - 5.1wt%, 0.6wt% - 3.2wt%, 0.4wt% - 2.5wt%, respectively (Table S2). The limit of detection (3*s*) (wt%) in IPA, acetone, THF, EtAC and ethanol is 0.085, 0.022, 0.026,

0.006, and 0.034, respectively (Figure S29-S33, Table S2), which is comparable to or better than those obtained by other fluorescent probes (Table S3). The relative standard deviation for 10 replicates detections of 1.27% water in IPA, acetone, THF, EtAC and ethanol is 0.10%, 0.06%, 0.10%, 0.24% and 0.03%, respectively, indicating the high precision of our method. Owing to the high stability of the COF in organic solvents, the prepared COF can be recycled to use in practice for the relative standard deviation of 8 recycling detections of water in analytical regent (AR) EtAc is 4.1% (Figure S34). To prove the accuracy of our method, we compared the results of the six commercial AR organic solvents tested with TzDa to those obtained by gas chromatography. The results show no obvious difference found between our method and gas chromatography, indicating the high reliability of our method (Table S4). All of the above results reveal the prepared COF is promising as a ratiometric fluorescence probe for rapid sensing of trace water in organic solvents.

CONCLUSIONS

We have reported the first example of high crystallinity of COFs with dual fluorescence emissions for ratiometric fluorescent sensing application. Rational design and synthesis of the new high crystallinity COF TzDa have been realized via a combined approach of introducing both docking sites and hydrogen bonds. The ligand Tz brings the docking sites and ICT effect to the TzDa, while the ligand Da offers the hydrogen bonds and ESIPT effect to the TzDa. The synergetic effect of docking sties and hydrogen bonds gives a high crystallinity AA eclipsed 2D layered COF with high thermal and chemical stability. Moreover, the introduction of ICT and the ESIPT

effects to TzDa brings dual fluorescence emissions of TzDa. The good stability and sensitive fluorescence response make TzDa great potential for building a ratiometric fluorescent sensor for trace water in organic solvents with quick response, low LOD, excellent accuracy, reproducibility and reusability. This work not only proposes a platform for the construction of high crystallinity COFs with dual fluorescence emissions, but also paves the way to the utilization of COFs for ratiometric fluorescent sensing application.

ASSOCIATED CONTENT

Supporting Information

The Supporting Information is available free of charge on the ACS Publications website at DOI: xxxxxx.

Additional materials and methods, Figures S1-S34 and Tables S1-S4 (PDF)

ACKNOWLEDGMENTS

- XPY appreciates the support from the National Basic Research Program of China (grant no. 2015CB932001), the National Natural Science Foundation of China (grant no 21435001), the Fundamental Research Funds for Central Universities (grant no. JUSRP51714B), and Open Funds of the State Key Laboratory of Electroanalytical Chemistry (SKLEAC201705).

REFERENCES

(1) Cote, A. P.; Benin, A. I.; Ockwig, N. W.; O'Keeffe, M.; Matzger, A. J.; Yaghi, O. M. Porous, Crystalline, Covalent Organic Frameworks. *Science* **2005**, *310*, 1166-1170.

(2) Feng, X.; Ding, X.; Jiang, D. Covalent Organic Frameworks. *Chem. Soc. Rev.* **2012**, *41*, 6010-6022.

(3) Ding, S. Y.; Wang, W. Covalent Organic Frameworks (COFs): from Design to Applications. *Chem. Soc. Rev.* **2013**, *42*, 548-568.

(4) Waller, P. J.; Gandara, F.; Yaghi, O. M. Chemistry of Covalent Organic Frameworks. *Acc. Chem. Res.* **2015**, *48*, 3053-3063.

(5) Segura, J. L.; Mancheno, M. J.; Zamora, F. Covalent Organic Frameworks Based on Schiff-base Chemistry: Synthesis, Properties and Potential applications. *Chem. Soc. Rev.* **2016**, *45*, 5635-5671.

(6) Kandambeth, S.; Mallick, A.; Lukose, B.; Mane, M. V.; Heine, T.; Banerjee, R. Construction of Crystalline 2D Covalent Organic Frameworks with Remarkable Chemical (acid/base) Stability via a Combined Reversible and Irreversible Route. *J. Am. Chem. Soc.* **2012**, *134*, 19524-19527.

(7) Chandra, S.; Kandambeth, S.; Biswal, B. P.; Lukose, B.; Kunjir, S. M.; Chaudhary, M.; Babarao, R.; Heine, T.; Banerjee, R. Chemically Stable Multilayered Covalent Organic Nanosheets from Covalent Organic Frameworks via Mechanical Delamination. *J. Am. Chem. Soc.* **2013**, *135*, 17853-17861.

(8) El-Kaderi, H. M.; Hunt, J. R.; Mendoza-Cortes, J. L.; Cote, A. P.; Taylor, R. E.; O'Keeffe, M.; Yaghi, O. M. Designed Synthesis of 3D Covalent Organic Framework. *Science* **2007**, *316*, 268-272.

(9) Zhang, Y. B.; Su, J.; Furukawa, H.; Yun, Y.; Gandara, F.; Duong, A.; Zou, X.; Yaghi, O. M. Single-crystal Structure of a Covalent Organic Framework. *J. Am. Chem. Soc.* **2013**, *135*, 16336-16339.

(10) Uribe-Romo, F. J.; Hunt, J. R.; Furukawa, H.; Klöck, C.; O'Keeffe, M.; Yaghi, O. M. A Crystalline Imine-linked 3-D Porous Covalent Organic Framework

(COF-300). *J. Am. Chem. Soc.* **2009**, *131*, 4570-4571.

(11) Liu, Y.; Ma, Y.; Zhao, Y.; Sun, X.; Gándara, F.; Furukawa, H.; Liu, Z.; Zhu, H.; Zhu, C.; Suenaga, K. Weaving of Organic Threads into a Crystalline Covalent Organic Framework. *Science* **2016**,*351*, 365-369.

(12) Ding, S. Y.; Gao, J.; Wang, Q.; Zhang, Y.; Song, W. G.; Su, C. Y.; Wang, W. Construction of Covalent Organic Framework for Catalysis: Pd/COF-LZU1 in Suzuki-Miyaura Coupling Reaction. *J. Am. Chem. Soc.* **2011**, *133*, 19816-19822.

(13) Xu, H.; Gao, J.; Jiang, D. Stable, Crystalline, Porous, Covalent Organic Frameworks as a Platform for Chiral Organocatalysts. *Nat.Chem.***2015**, *7*, 905-912.

(14) Wang, Bhadra, M.; Sasmal, H. S.; Basu, A.; Midya, S. P.; Kandambeth, S.; Pachfule, P.; Balaraman, E.; Banerjee, R. Predesigned Metal-Anchored Building Block for In Situ Generation of Pd Nanoparticles in Porous Covalent Organic Framework: Application in Heterogeneous Tandem Catalysis. *ACS Appl. Mater. Inter.* **2017**, *9*, 13785-13792.

(15) Chen, L.; Furukawa, K.; Gao, J.; Nagai, A.; Nakamura, T.; Dong, Y.; Jiang, D. Photoelectric Covalent Organic Frameworks: Converting Open Lattices into Ordered Donor-acceptor Heterojunctions. *J. Am. Chem. Soc.* **2014**, *136*, 9806-9809.

(16) Huang, N.; Ding, X.; Kim, J.; Ihee, H.; Jiang, D. A Photoresponsive Smart Covalent Organic Framework. *Angew. Chem. Int. Ed.* **2015,** *54*, 8704-8707.

(17) Yang, H.; Zhang, S.; Han, L.; Zhang, Z.; Xue, Z.; Gao, J.; Li, Y.; Huang, C.; Yi, Y.; Liu, H.; Li, Y. High Conductive Two-Dimensional Covalent Organic Framework for Lithium Storage with Large Capacity. *ACS Appl. Mater. Inter.* **2016**, *8*, 5366-5375.

(18) Wang, H.; Li, B.; Wu, H.; Hu, T. L.; Yao, Z.; Zhou, W.; Xiang, S.; Chen, B. A Flexible Microporous Hydrogen-Bonded Organic Framework for Gas Sorption and

Separation. *J. Am. Chem. Soc.* **2015,** *137*, 9963-9970.

(19) Furukawa, H.; Yaghi, O. M. Storage of Hydrogen, Methane, and Carbon Dioxide in Highly Porous Covalent Organic Frameworks for Clean Energy Applications. *J. Am. Chem. Soc.* **2009,** *131*, 8875-8883.

(20) Baldwin, L. A.; Crowe, J. W.; Pyles, D. A.; McGrier, P. L. Metalation of a Mesoporous Three-Dimensional Covalent Organic Framework. *J. Am. Chem. Soc.* **2016,** *138*, 15134-15137.

(21) Yang, C. X.; Liu, C.; Cao, Y. M.; Yan, X. P. Facile Room-temperature Solution-phase Synthesis of a Spherical c Covalent Organic Framework for High-resolution Chromatographic Separation. *Chem. Commun.* **2015,** *51*, 12254-12257.

(22) Qian, H.-L.; Yang, C.-X.; Yan, X.-P. Bottom-up Synthesis of Chiral Covalent Organic Frameworks and Their Bound Capillaries for Chiral Separation. *Nat. Commun.* **2016**, *7*, 12104.

(23) Ding, S. Y.; Dong, M.; Wang, Y. W.; Chen, Y. T.; Wang, H. Z.; Su, C. Y.; Wang, W. Thioether-based Fluorescent Covalent Organic Framework for Selective Detection and Facile Removal of Mercury (II). *J. Am. Chem. Soc.* **2016**, *138*, 3031-3037.

(24) Huang, N.; Zhai, L.; Xu, H.; Jiang, D. Stable Covalent Organic Frameworks for Exceptional Mercury Removal from Aqueous Solutions. *J. Am. Chem. Soc.* **2017**, *139*, 2428-2434.

(25) Kandambeth, S.; Shinde, D. B.; Panda, M. K.; Lukose, B.; Heine, T.; Banerjee, R. Enhancement of Chemical Stability and Crystallinity in Porphyrin-containing Covalent Organic Frameworks by Intramolecular Hydrogen Bonds. *Angew. Chem. Int. Ed.* **2013**, *52*, 13052-13056.

(26) Kandambeth, S.; Venkatesh, V.; Shinde, D. B.; Kumari, S.; Halder, A.; Verma, S.; Banerjee, R. Self-templated Chemically Stable Hollow Spherical Covalent Organic Framework. *Nat.Commun.* **2015**, *6*, 6786.

(27) Ascherl, L.; Sick, T.; Margraf, J. T.; Lapidus, S. H.; Calik, M.; Hettstedt, C.; Karaghiosoff, K.; Döblinger, M.; Clark, T.; Chapman, K. W.; Auras, F.; Bein, T. Molecular Docking Sites Designed for the Generation of Highly Crystalline Covalent Organic Frameworks. *Nat. Chem.* **2016**, *8*, 310-316.

(28) Halder, A.; Kandambeth, S.; Biswal, B. P.; Kaur, G.; Roy, N. C.; Addicoat, M.; Salunke, J. K.; Banerjee, S.; Vanka, K.; Heine, T.; Verma, S.; Banerjee, R. Decoding the Morphological Diversity in Two Dimensional Crystalline Porous Polymers by Core Planarity Modulation. *Angew. Chem. Int. Ed.* **2016**, *55*, 7806-7810.

(29) Chen, X.; Huang, N.; Gao, J.; Xu, H.; Xu, F.; Jiang, D. Towards Covalent Organic Frameworks with Predesignable and Aligned Open Docking Sites. *Chem. Commun.* **2014**, *50*, 6161-6163.

(30) Kumar, P.; Kaushik, R.; Ghosh, A.; Jose, D. A. Detection of Moisture by Fluorescent off-on Sensor in Organic Solvents and Raw Food Products. *Anal. Chem.* **2016**, *88*, 11314-11318.

(31) Jung, H. S.; Verwilst, P.; Kim, W. Y.; Kim, J. S. Fluorescent and Colorimetric Sensors for the Detection of Humidity or Water Content. *Chem. Soc. Rev.* **2016**, *45*, 1242-1256.

(32) Huang, Y.; Liu, W.; Feng, H.; Ye, Y.; Tang, C.; Ao, H.; Zhao, M.; Chen, G.; Chen, J.; Qian, Z. Luminescent Nanoswitch Based on Organic-Phase Copper Nanoclusters for Sensitive Detection of Trace Amount of Water in Organic Solvents. *Anal. Chem.* **2016**, *88*, 7429-7434.

(33) Dong, Y.; Cai, J.; Fang, Q.; You, X.; Chi, Y. Dual-Emission of Lanthanide

Metal–Organic Frameworks Encapsulating Carbon-Based Dots for Ratiometric Detection of Water in Organic Solvents. *Anal. Chem.* **2016**, *88*, 1748–1752

(34) Dai, C.; Yang, C.-X.; Yan, X.-P. Ratiometric Fluorescent Detection of Phosphate in Aqueous Solution Based on Near Infrared Fluorescent Silver Nanoclusters/Metal–Organic Shell Composite. *Anal. Chem.* **2015**, *87*, 11455-11459.

(35) Xu, F.; Xu, H.; Chen, X.; Wu, D.; Wu, Y.; Liu, H.; Gu, C.; Fu, R.; Jiang, D. Radical Covalent Organic Frameworks: a General Strategy to Immobilize Open-Accessible Polyradicals for High-Performance Capacitive Energy Storage. *Angew. Chem. Int. Ed.* **2015**, *54*, 6814-6818.

(36) Huang, N.; Chen, X.; Krishna, R.; Jiang, D. Two-dimensional Covalent Organic Frameworks for Carbon Dioxide Capture through Channel-Wall Functionalization. *Angew. Chem. Int. Ed.* **2015**, *54*, 2986-2990.

(37) Smith, B. J.; Overholts, A. C.; Hwang, N.; Dichtel, W. R. Insight into the Crystallization of Amorphous Imine-Linked Polymer Networks to 2D Covalent Organic Frameworks. *Chem. Commun.* **2016**, *52*, 3690-3693.

(38) Kang, Z.; Peng, Y.; Qian, Y.; Yuan, D.; Addicoat, M. A.; Heine, T.; Hu, Z.; Tee, L.; Guo, Z.; Zhao, D. Mixed Matrix Membranes (MMMs) Comprising Exfoliated 2D Covalent Organic Frameworks (COFs) for Efficient CO_2 Separation. *Chem. Mater.* **2016**, *28*, 1277−1285.

(39) Cole, H. Bragg's Law and Energy Sensitive Detectors. *J. Appl. Crystallogr*. **1970**, *3*, 405-406.

(40) Gomes, R.; Bhanja, P.; Bhaumik, A. A Triazine-based Covalent Organic Polymer for Efficient CO_2 Adsorption. *Chem. Commun.* **2015**, *51*, 10050-10053.

(41) Nandi, S.; Mandal, S.; Matalobos, J. S.; Sahana, A.; Das, D. Interaction of Water with a Benzimidazole Derivative: Fluorescence and Colorimetric Recognition

of Trace Level Water Involving Intra−Molecular Charge Transfer Process. *J. Mol. Recognit.* **2015**, *29*, 5-9.

(42) Niu, C. G.; Guan, A. L.; Zeng, G. M.; Liu, Y. G.; Li, Z. W. Fluorescence Water Sensor Based on Covalent Immobilization of Chalcone Derivative. *Anal. Chim. Acta* **2006**, *577*, 264-270.

(43) Jung, H. S.; Verwilst, P.; Kim, W. Y.; Kim, J. S. Fluorescent and Colorimetric Sensors For the Detection of Humidity or Water Content. *Chem. Soc. Rev.* **2016**, *45*, 1242-1256.

(44) Lee, M. H.; Kim, J. S.; Sessler, J. L. Small Molecule-Based Ratiometric Fluorescence Probes for Cations, Anions, and Biomolecules. *Chem. Soc. Rev.* **2015**, *44*, 4185-4191.

(45) Zhao, J.; Ji, S.; Chen, Y.; Guo, H.; Yang, P. Excited State Intramolecular Proton Transfer (Esipt): from Principal Photophysics to the Development of New Chromophores and Applications in Fluorescent Molecular Probes and Luminescent Materials. *Phys. Chem. Chem. Phys.* **2012**, *14*, 8803-8817.

(46) Niu, C. G.; Qin, P. Z.; Zeng, G. M.; Gui, X. Q.; Guan, A. L. Fluorescence Sensor for Water in Organic Solvents Prepared from Covalent Immobilization of 4-morpholinyl-1, 8-naphthalimide. *Anal. Bioanal. Chem.* **2007**, *387*, 1067-1074.

TOC

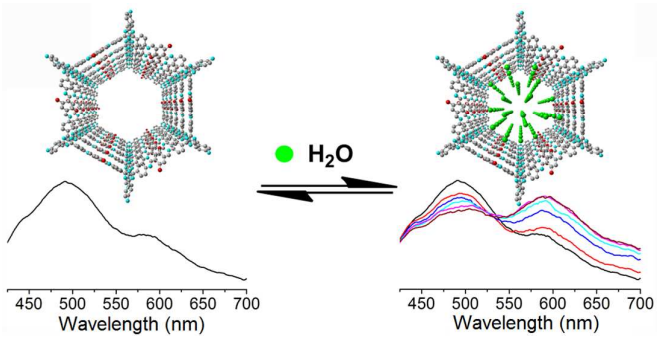
H2O
450 500 550 600 650 700
Wavelength (nm)
450 500 550 600 650 700
Wavelength (nm)